short communications

Surface-entropy reduction used in the crystallization of human choline acetyltransferase

Ae-Ri Kim,[a] Tomas Dobransky,[b] R. Jane Rylett[b,c] and Brian H. Shilton[a]*

[a]Department of Biochemistry, University of Western Ontario, London, Ontario N6A 5C1, Canada, [b]Robarts Research Institute, London, Ontario N6A 5C1, Canada, and [c]Department of Physiology and Pharmacology, University of Western Ontario, London, Ontario N6A 5C1, Canada

Correspondence e-mail: bshilton@uwo.ca

Human choline acetyltransferase (ChAT) synthesizes the neurotransmitter acetylcholine (ACh) from choline and acetyl-CoA. A crystal structure of human ChAT has been a long-standing goal in the neuronal signalling field. Milligram quantities of pure ChAT can be purified [Kim *et al.* (2005), *Protein Expr. Purif.* **40**, 107–117], but exhaustive crystallization efforts failed to produce any crystals suitable for high-resolution structural studies. To obtain high-quality crystals of human ChAT, a truncation was made in a large poorly conserved loop region and high-entropy side chains were removed from the surface of the protein. The resulting 'entropy-reduced' ChAT (MR = 68.1 kDa) crystallizes readily and reproducibly and the crystals diffract X-rays to approximately 2.2 Å. The availability of these crystals will allow us to study the structure of human ChAT on its own as well as in complex with its substrates and inhibitor molecules, leading to a greater understanding of its catalytic mechanism and regulation.

1. Introduction

Neurochemical communication between cholinergic neurons and their targets is dependent on the activity of choline acetyltransferase (EC 2.3.1.6; ChAT), which catalyzes the transfer of an acetyl group from acetyl-CoA to choline to form the transmitter acetylcholine (ACh). Decreased ChAT activity is found in several neurological and psychological disorders, such as Alzheimer's disease (Whitehouse, 1998) and schizophrenia (Holt *et al.*, 1999; Wu *et al.*, 1993). Crystals of *Drosophila* ChAT were reported over 12 years ago (Wu *et al.*, 1993), but only recently has rat ChAT has been crystallized and its structure solved (Cai *et al.*, 2004; Govindasamy *et al.*, 2004; Lian *et al.*, 2004), suggesting that there were difficulties in obtaining suitable crystals of the enzyme. Our efforts have been directed towards structure determination of human ChAT, but obtaining diffraction-quality crystals has proven to be extremely difficult. We developed two different purification methods to obtain large quantities of pure human ChAT and removed residues at the carboxyl-terminus of the protein that we found were prone to proteolysis (Kim *et al.*, 2005). Although removal of these carboxyl-terminal residues may have facilitated crystallization, crystals still appeared only sporadically and diffracted poorly, probably owing to their small size. Human ChAT is highly susceptible to oxidation, resulting in rapid loss of catalytic activity and the formation of intermolecular disulfide bonds (Kim *et al.*, 2005). However, crystallization screens in the presence of reducing agents and/or under an argon atmosphere were not successful.

To improve the ability of human ChAT to form ordered crystals, we used 'surface-entropy reduction', a method described by Derewenda (2004). The basis of the method is to reduce the entropic cost of crystallization by removal of disordered side chains that project from the surface of the molecule and replacement with alanine. In addition, we deleted several residues in a large non-conserved loop. These changes to the enzyme led to a small reduction in its stability, but its catalytic activity was retained. 'Entropy-reduced' human ChAT (ER-ChAT; 612 residues, 68.1 kDa) begins to form crystals within minutes of being mixed with polyethylene glycol (PEG) solutions and the crystals diffract to high resolution.

2. Materials and methods

All buffers and salts were analytical grade obtained from Sigma, BDH or J. T. Baker. PEGs used for crystallization were from Fluka.

Table 1
Choline acetyltransferase expression vectors and crystallization results.

No.	Plasmid	Protein expressed	Crystallization
1	pChAT	Wild-type; 70 kDa untagged ChAT purified by immunoaffinity chromatography (Dobransky et al., 2001)	Small rod-shaped crystals, not reproducible
2	pProEX-ChAT	His$_6$-ChAT; wild-type 70 kDa ChAT with cleavable hexahistidine-affinity tag (Kim et al., 2005)	Sporadic small crystals (Fig. 1a)
3	pProEX-ChATΔ615	His$_6$-ChATΔ615; C-terminus truncated by 15 residues (Kim et al., 2005)	Sporadic small crystals (Fig. 1a)
4	pChAT-225	His$_6$-ChATΔ615 with mutations E225A, D226A and E227A	Not tested
5	pChAT-518	His$_6$-ChATΔ615 with mutations K518A and E519A	Not tested
6	pChAT-582	His$_6$-ChATΔ615 with mutations K582A and E583A	Not tested
7	pChAT-518/582	His$_6$-ChATΔ615 with mutations K518A, E519A, K582A and E583A	Not tested
8	pChAT-Δloop10	His$_6$-ChATΔ615 with residues 346–358 replaced with the sequence PELVRSPMVP	Not tested
9	pChAT-Δloop8	His6-ChATΔ615 with residues 346–358 replaced with the sequence PLVRPMVP	Not tested
10	pChAT-ER	ER-ChAT; His$_6$-ChATΔ615 with mutated regions E225A/D226A/E227A, K518A/E519A and K582A/E583A, along with the loop change in pChAT-Δloop10	Large well ordered crystals obtained reproducibly (Fig. 1b)
11	pChAT-ER8	ER8-ChAT; His$_6$-ChATΔ615 with mutated regions E225A/D226A/E227A, K518A/E519A and K582A/E583A, along with the loop change in pChAT-Δloop8	Not tested (poor expression)

2.1. Mutagenesis

Entropy-reducing mutations were introduced into ChAT by site-directed mutagenesis using the QuikChange kit (Stratagene) along with primers designed according to the directions in the kit. Vectors are listed in Table 1. The template used for mutagenesis was pProEX-ChATΔ615, which encodes the carboxyl-terminal truncated version of human ChAT, fused at its amino-terminus to a hexahistidine affinity tag (Kim et al., 2005). Changes from high-entropy residues to alanine were made in three regions, E225A/D226A/E227A, K518A/E519A and K582A/E583A, to produce plasmids pChAT-225, pChAT-518 and pChAT-582.

A putative disordered loop region in human ChAT, spanning 13 residues from 346 to 358, was replaced with a shorter ten-residue sequence from human carnitine acetyltransferase (CrAT; residues 365–375). The loop deletion/mutagenesis was carried out using a two-step nested PCR protocol to produce a PCR fragment containing the deletion/mutation with flanking NarI and SmaI restriction sites; this PCR product was digested with NarI and SmaI and ligated into pProEX-ChATΔ615 to produce pChAT-Δloop10. A related construct, pChAT-Δloop8, was also made in which an additional two residues were deleted from the loop (Table 1).

The three sets of entropy-reducing mutations were combined with each of the two loop truncations to produce two constructs: ER-ChAT, which contains the ten-residue loop, and ER8-ChAT, containing the eight-residue loop (Table 1). To produce vectors coding for these proteins, plasmid pChAT-518/582, carrying mutations K518A, E519A, K582A and E583A, was generated by sequential QuikChange mutagenesis. The fragment harbouring the mutations was isolated by digestion with SmaI and BamHI followed by gel purification and ligation into pChAT-Δloop10 and pChAT-Δloop8. Finally, a restriction fragment containing the E225A/D226A/E227A mutations was isolated from pChAT-225 by digestion with NarI and Eco47III, gel-purified and ligated into the vectors to produce pChAT-ER and pChAT-ER8 (Table 1). The ChAT coding region in these plasmids was sequenced to verify the presence of the mutations and sequence integrity.

2.2. Purification and crystallization

Crystals of human ChAT were originally obtained from the native wild-type 70 kDa recombinant protein purified by immunoaffinity chromatography as described previously (Dobransky et al., 2001).

Prior to crystallization, immunoaffinity-purified ChAT (IP-ChAT) was exchanged into 20 mM Tris pH 8.5 by gel-filtration chromatography (Superdex 200 HP, 1 × 30 cm) and concentrated by evaporation in vacuo to 10 mg ml^{-1}.

Human ChAT was expressed as a fusion with an amino-terminal hexahistidine-affinity tag and purified as described previously (Kim et al., 2005). Note that the affinity tag was removed by specific proteolysis prior to crystallization trials. The same expression and purification methodology was used for ChATΔ615 (a construct lacking the extreme carboxyl-terminal 15 amino acids) and ER-ChAT. Prior to crystallization, purified wild-type ChAT (WT-ChAT) or ChATΔ615 was dialyzed into 20 mM Tris pH 8.5, 500 mM NaCl, 10%(v/v) glycerol and 0.5 mM TCEP, whereas ER-ChAT was dialyzed into 20 mM Tris pH 8.5, 100 mM NaCl, 10%(v/v) glycerol and 0.5 mM TCEP.

Screening for crystallization conditions was conducted using Wizard Screens I and II (Emerald Biosciences) and/or Crystal Screens I and II (Hampton Research). Crystallization screens were carried out by sitting-drop vapour diffusion with VDX plates (Hampton Research) or Compact Clover plates (Emerald Biosciences).

2.3. X-ray data collection and processing

WT-ChAT crystals grown in MgSO$_4$ were cryoprotected by soaking in a solution containing the reservoir components and 30%(v/v) glycerol. The crystals were mounted in a nylon loop (Hampton Research) and flash-frozen in a nitrogen-gas stream at 100 K. Data were collected at the National Synchrotron Light Source (NSLS) beamline X8C (λ = 1.1 Å) using an ADSC Quantum 4R CCD detector system with a crystal-to-detector distance of 300 mm, an oscillation angle of 1° and an exposure time of 40 s.

ER-ChAT crystals grown from PEG solutions were cryoprotected by soaking the crystals in a solution containing 10%(w/v) PEG 3350, 100 mM Tris pH 8.5 and 25%(v/v) glycerol. Data were collected in-house using a Rigaku RUH3R rotating-anode X-ray generator (λ = 1.5418 Å) with a MAR 345 image-plate detector, with a crystal-to-detector distance of 200 mm, an 0.5° oscillation angle and an exposure time of 400 s per image. All data were indexed, processed and merged using the HKL suite (Otwinowski, 1991).

2.4. Measurement of thermal denaturation rate

To determine thermal denaturation rate constants for WT-ChAT, ChATΔ615 and ER-ChAT, the enzymes were incubated at selected temperatures where significant thermal denaturation takes place. After a fixed time interval, aliquots were removed and stabilized at 277 K; the amount of active (non-denatured) enzyme was then determined by measuring the rate of the reverse reaction, namely synthesis of acetyl-CoA from CoA and ACh, using a coupled assay system (Hersh et al., 1978). The detailed procedure was as follows: 1.35 ml incubation buffer [20 mM Tris–HCl, 0.5 M NaCl, 10%(v/v) glycerol and 0.5 mM TCEP pH 8.5] was pre-incubated in a water bath at the temperatures indicated in Fig. 2 and 25 µg ChAT was added; at given time points, 80 µl aliquots were removed and mixed immediately with assay buffer (10 mM K_2HPO_4, 250 mM NaCl, 0.125 mM NAD^+, 0.5 mM malate, 0.5 mM DTT pH 7.4) pre-chilled to 277 K. To assay ChAT activity, 0.3 U citrate synthase, 0.8 U malate dehydrogenase and 0.2 mM CoA were mixed with the ChAT assay buffer and pre-incubated at 310 K for 15 min. The ChAT-catalyzed conversion of ACh and CoA to choline and acetyl-CoA was initiated by the addition of 10 mM ACh. For each time point, the rate of NADH production (which is directly proportional to the rate of ACh production by ChAT) was measured from the change in fluorescence at 460 nm (excitation wavelength 340 nm) using a Victor3 plate reader (Perkin–Elmer). These rates were plotted against the time of incubation at denaturing temperature and the curves were fitted to a first-order reaction to obtain rate constants for ChAT inactivation.

3. Results and discussion

Our first crystals of human ChAT were obtained from protein that had been purified by immunoaffinity chromatography (IP-ChAT; Table 1). Several simple screens using either ammonium sulfate or PEG at varying pH values resulted in the appearance of tiny rod-like crystals of IP-ChAT from solutions containing 2.7 M ammonium sulfate, 100 mM NaCl, 100 mM glycine pH 3.5. The crystals were rod-shaped and smaller than 50 µm in the longest dimension and appeared over a period of 2–3 weeks; the crystals were too small for diffraction analysis and we were unable to reproduce the crystallization to increase their size.

Immunoaffinity chromatography could be used to produce only very limited quantities of pure ChAT. In order to search more broadly for suitable crystallization conditions, we developed alternative purification procedures (Kim et al., 2005). For most of our crystallization trials, we used human ChAT that had been expressed as a hexahistidine-tagged construct: the protein was purified by Ni^{2+}-affinity chromatography followed by removal of the affinity tag and a final cation-exchange chromatography step. This protein crystallized sporadically from solutions of approximately 1.5 M magnesium sulfate at pH 3.5, conditions similar to those from which IP-ChAT crystallized. The crystals obtained had a bipyramidal morphology and were never larger than 50 µm in any dimension (Fig. 1a). Diffraction from these crystals was too weak to measure using our home source, but we were able to collect a data set at a synchrotron source (beamline X8C at the Brookhaven National Laboratory). Unfortunately, only the stronger reflections were visible (Fig. 1a), consistent with the extremely low overall average $I/\sigma(I)$ of the data set (Table 2). Note that the protein had a relatively large unit cell with two molecules per asymmetric unit, corresponding to a solvent content of 48%. These crystals appeared promising and we collected data using a more brilliant synchrotron beamline (Cornell High Energy Synchrotron Source, beamline A1), but could not obtain a suitable

data set. Our efforts to grow larger more strongly diffracting crystals were unsuccessful, primarily because crystallization was infrequent and unpredictable. Through the course of these additional crystallization trials, we discovered that 15 carboxyl-terminal residues were
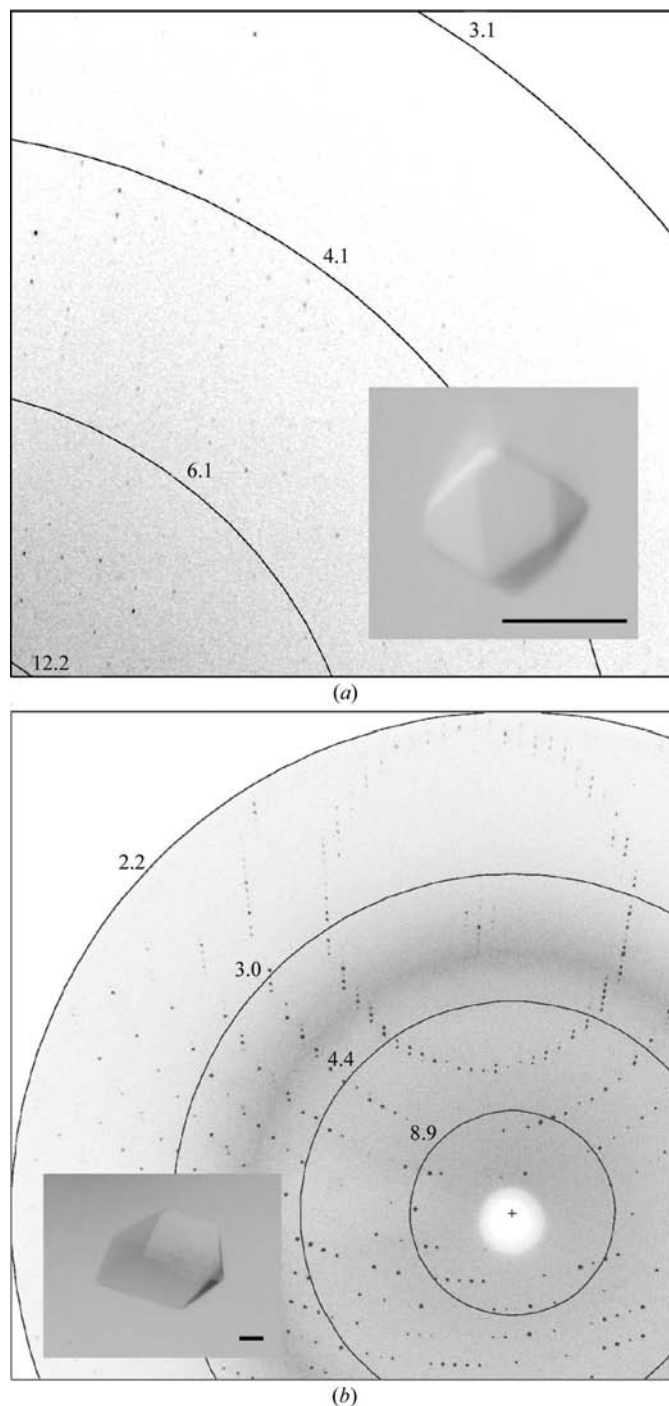

Figure 1
Diffraction from human ChAT Crystals. (a) Diffraction from a crystal of wild-type ChAT was recorded at beamline X8C, NSLS. ChAT or ChATΔ615 was purified using a His_6-affinity tag as described previously (Kim et al., 2005) and in both cases bipyramid-shaped crystals (inset, with the scale bar representing 50 µm) appeared sporadically from solutions of magnesium sulfate pH 3.5. Diffraction from these crystals extended to beyond 4 Å, but was extremely weak, with only the strongest reflections visible. (b) Entropy-reduced ChAT (ER-ChAT) crystallizes readily from PEG solutions at pH 8.5 to form large crystals (inset, with the scale bar representing 100 µm) that diffract X-rays to beyond 2.2 Å using a rotating-anode source.

Table 2
Data-collection statistics for ChAT crystals.

Values in parentheses refer to the highest resolution shell.

Parameter	WT-ChAT†	ER-ChAT‡
Space group	$I422$	$P2_12_12_1$
Unit-cell parameters (Å)	$a = b = 155.95$,	$a = 54.74$, $b = 75.75$,
	$c = 220.57$	$c = 165.69$
Resolution (Å)	100–4.0 (4.14–4.00)	40–2.25 (2.33–2.25)
Total reflections§	116375	165572
Unique reflections	11050	32874
Redundancy	10.6 (10.6)	5.0 (4.3)
Completeness§ (%)	93.3 (95.0)	97.9 (96.4)
$\langle I/\sigma(I)\rangle$	9.2 (6.4)	26.5 (12.1)
R_{merge} (%)	22.4 (31.5)	3.8 (9.3)

† Data collected at NSLS beamline X8C, New York, USA; $\lambda = 1.1$ Å.   ‡ Data collected using a rotating-anode generator; $\lambda = 1.5418$ Å.   § Only reflections with $I > \sigma(I)$ were considered.

susceptible to proteolysis. We therefore constructed a carboxyl-terminal truncated version of human ChAT, 'ChATΔ615', and found that this protein produced crystals more frequently than the full-length version; however, even for ChATΔ615, crystallization was sporadic and the crystals were too small for diffraction analysis.

Human ChAT contains a large number of cysteine residues and the sporadic nature of its crystallization, as well as the fact that crystals only appeared after 2–4 weeks, led us to think that cysteine oxidation may be a factor. Trials were conducted under an argon atmosphere in the presence of TCEP, a strong reducing agent, but crystals were not produced under these conditions. We also attempted to alter the surface properties and crystallization behaviour of human ChAT by reductive methylation of amino groups (Rayment, 1997). Reductively methylated ChAT was subjected to extensive crystallization trials but failed to produce crystals under any of the conditions tested.

We then turned our attention to other features of the enzyme that might cause problems with crystallization. Human ChAT contains an internal region, residues 346–358, that is susceptible to proteolysis (Wu et al., 1995). In the crystal structure of rat ChAT (Cai et al., 2004), the corresponding residues are in a large surface-exposed loop with atomic B factors exceeding 100 Å^2, indicating that the loop is highly mobile. Poorly structured and conformationally flexible regions can interfere with crystallization and therefore one of our goals was to engineer human ChAT with a truncated and less mobile loop. Carnitine acetyltransferase (CrAT) is a closely related enzyme the crystal structure of which has been solved (Jogl & Tong, 2003). In CrAT, the loop in question is three residues shorter than in human ChAT. Based on sequence alignment and predicted structural similarity between human CrAT and ChAT, we replaced 13 residues from the ChAT loop, 346-SSRKLIRADSVSE-358, with ten residues (365-PELVRSPMVP-375) from the corresponding region of human CrAT to produce ChAT-Δloop10. We also truncated the loop by an additional two residues, replacing the 13-residue ChAT loop with the eight-residue sequence -PLVRPMVP- to create ChAT-Δloop8. Both ChAT-Δloop10 and ChAT-Δloop8 were expressed at levels comparable to the wild-type protein and crude cell extracts had similar levels of ChAT activity (data not shown).

To further increase the probability of obtaining suitable crystals of human ChATΔ615, we incorporated entropy-reducing mutations into human ChAT, following guidelines described by Derewenda (2004). Ultimately, we planned to combine entropy-reducing point mutations with the loop truncations in ChAT-Δloop10 and ChAT-Δloop8. The homology model of human ChAT (based on the co-ordinates of the rat enzyme; PDB code 1q6x; Cai et al., 2004) was examined for regions that are structurally immobile, project away from the surface of the protein and contain lysine and/or glutamic

acid: three regions were found which, upon mutation of the 'high-entropy' residues to alanine, would provide potential crystal contacts. Site-directed mutagenesis was used to produce three constructs from which the following ChAT proteins could be expressed: ChAT-E225A/D226A/E227A, ChAT-K518A/E519A and ChAT-K582A/E583A. All three proteins were expressed to wild-type levels in an E. coli background and crude cell extracts had ChAT activities that were similar to the wild-type protein (data not shown).

From the work outlined above, we knew that none of the individual changes, neither the two loop insertion/deletions nor the three sets of entropy-reducing mutations, appeared to have a fatal effect on the folding or function of ChAT. Therefore, we combined these mutations into two ChAT constructs, ER-ChAT and ER8-ChAT. Both constructs harbour entropy-reducing mutations in the three regions described above, but ER-ChAT has the ten-residue loop while ER8-ChAT has the eight-residue loop. Note that these constructs are based on ChATΔ615 and thus they also lack the carboxyl-terminal 15 residues (Table 1).

ER-ChAT and ER8-ChAT were both expressed at wild-type levels and both proteins could be purified using an identical protocol to the wild-type protein. However, we found that the yield of ER8-ChAT was low (1 or 2 mg from 4 l culture), indicating that the protein was probably not stable, and so we did not continue to use this construct. On the other hand, the yield of ER-ChAT was almost as high as that of the wild-type protein (approximately 12 mg of ER-ChAT per 4 l culture, compared with 15 mg for the wild type).

Once purified, it was obvious that the mutations in ER-ChAT had a dramatic effect on its ability to crystallize. Crystals of ER-ChAT were initially observed from solutions of 15%(w/v) PEG 3000 and 50 mM CHES pH 9.5. Several systematic crystallization screens indicated that the optimal conditions consisted of 10–13%(w/v) PEG 3350 at pH 8.5 and 277 K. Under these conditions, ER-ChAT crystals begin to form almost immediately upon mixing with the reservoir solution and the crystals grew reproducibly to a large size (Fig. 1b). Crystals of ER-ChAT have a low mosaic spread, one molecule per asymmetric unit (solvent content of 51%) and diffract X-rays to beyond 2.2 Å resolution using a rotating-anode source (Fig. 1 and Table 2).
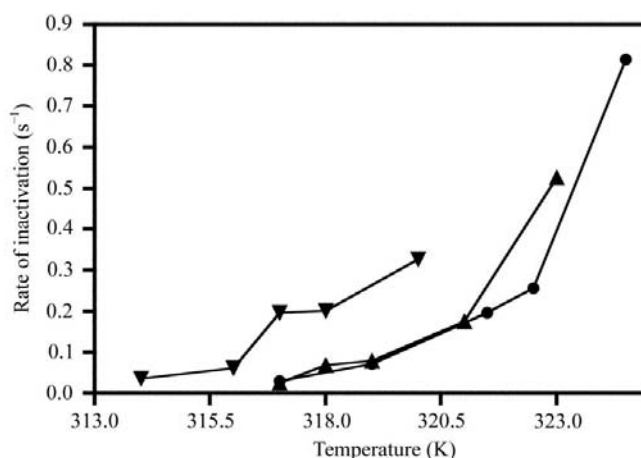

Figure 2
Thermal denaturation of ChAT and ER-ChAT. Proteins were incubated at temperatures where there was a significant rate of thermal denaturation. Aliquots were removed at various time points and stabilized in buffer at 277 K; ChAT activity was then measured and the decrease in activity was fitted to a first-order reaction to yield a rate constant for denaturation. Filled circles represent wild-type ChAT and filled triangles represent ChATΔ615, which is identical to wild-type ChAT except that 15 residues were removed from the carboxyl-terminus of the protein. The inverted triangles represent entropy-reduced ChAT (ER-ChAT), which is ChATΔ615 with a truncated loop region as well as mutations that reduce surface entropy in three other regions of the protein (Table 1).

The specific activity of ER-ChAT is 50.9 µmol min^{-1} mg^{-1}, which is essentially identical to that of the wild-type enzyme (Kim *et al.*, 2005); therefore, structural studies of the protein in complex with its substrates and inhibitors will be physiologically meaningful. Results from the crystallization trials indicated that ER-ChAT is significantly less soluble than the parent enzyme, as one would expect given that charged surface residues have been substituted for alanine. ER-ChAT is also less thermostable than the wild-type protein: rate constants for inactivation of ER-ChAT and wild-type ChAT at various temperatures are shown in Fig. 2, where it can be seen that at 317 K the rate of inactivation of ER-ChAT was approximately sevenfold greater than either wild-type ChAT or ChATΔ615. The basis for this destabilization is not clear, although it was anticipated based on previous studies (Mateja *et al.*, 2002). At any rate, the relatively small decrease in stability of the enzyme is considered to be acceptable given the dramatic improvement in crystallization.

Our choice of regions in ChAT that were good potential candidates for entropy reduction was facilitated by the availability of crystal structures of the homologous proteins, human CrAT and rat ChAT. Even in the absence of any structural information, short regions rich in lysine and glutamic acid and bracketed by conserved polypeptide can be identified from multiple sequence alignments (Derewenda, 2004). The possibility of exerting rational control over the crystallization process, coupled with the relative ease of site-directed mutagenesis, especially using procedures where more than one region can be mutated at a time (for example, using the QuikChange Multi kit from Stratagene), means that entropy-reducing mutagenesis should become a favourite in the protein crystallographer's toolbox. Certainly, the dramatic results we have obtained with human ChAT

have convinced us of the utility of the method and we will incorporate such changes in other structural targets at an early stage.

References

Cai, Y., Cronin, C. N., Engel, A. G., Ohno, K., Hersh, L. B. & Rodgers, D. W. (2004). *EMBO J.* **23**, 2047–2058.

Derewenda, Z. S. (2004). *Structure*, **12**, 529–535.

Dobransky, T., Davis, W. L. & Rylett, R. J. (2001). *J. Biol. Chem.* **276**, 22244–22250.

Govindasamy, L., Pedersen, B., Lian, W., Kukar, T., Gu, Y., Jin, S., Agbandje-McKenna, M., Wu, D. & McKenna, R. (2004). *J. Struct. Biol.* **148**, 226–235.

Hersh, L. B., Coe, B. & Casey, L. (1978). *J. Neurochem.* **30**, 1077–1085.

Holt, D. J., Herman, M. M., Hyde, T. M., Kleinman, J. E., Sinton, C. M., German, D. C., Hersh, L. B., Graybiel, A. M. & Saper, C. B. (1999). *Neuroscience*, **94**, 21–31.

Jogl, G. & Tong, L. (2003). *Cell*, **112**, 113–122.

Kim, A. R., Doherty-Kirby, A., Lajoie, G., Rylett, R. J. & Shilton, B. H. (2005). *Protein Expr. Purif.* **40**, 107–117.

Lian, W., Gu, Y., Pedersen, B., Kukar, T., Govindasamy, L., Agbandje-McKenna, M., Jin, S., McKenna, R. & Wu, D. (2004). *Acta Cryst.* D**60**, 374–375.

Mateja, A., Devedjiev, Y., Krowarsch, D., Longenecker, K., Dauter, Z., Otlewski, J. & Derewenda, Z. S. (2002). *Acta Cryst.* D**58**, 1983–1991.

Otwinowski, Z. (1991). *Proceedings of the CCP4 Study Weekend. Isomorphous Replacement and Anomalous Scattering*, edited by L. Sawyer, N. Isaacs & S. Bailey, pp. 56–62. Warrington: Daresbury Laboratory.

Rayment, I. (1997). *Methods Enzymol.* **276**, 171–179.

Whitehouse, P. J. (1998). *J. Clin. Psychiatry*, **59**, Suppl. 13, 19–22.

Wu, D., Ahmed, S. N., Lian, W. & Hersh, L. B. (1995). *J. Biol. Chem.* **270**, 19395–19401.

Wu, D., Schormann, N., Lian, W., Deisenhofer, J. & Hersh, L. B. (1993). *J. Neurochem.* **61**, 1416–1422.